Generation of spin-polarized current using multiterminal quantum dot with spin-orbit interaction

Tomohiro Yokoyama* and Mikio Eto

Faculty of Science and Technology, Keio University, 3-14-1 Hiyoshi, Kohoku-ku, Yokohama 223-8522, Japan

(Received 29 August 2012; published 6 November 2012)

We theoretically examine generation of spin-polarized current using multiterminal quantum dot with spin-orbit interaction. First, a two-level quantum dot is analyzed as a minimal model, which is connected to N ($\geqslant 2$) external leads via tunnel barriers. When an unpolarized current is injected to the quantum dot from a lead, a polarized current is ejected to others, similarly to the spin Hall effect. In the absence of magnetic field, the generation of spin-polarized current requires $N \geqslant 3$. The polarization is markedly enhanced by resonant tunneling when the level spacing in the quantum dot is smaller than the level broadening due to the tunnel coupling to the leads. In a weak magnetic field, the orbital magnetization creates a spin-polarized current even in the two-terminal geometry ($N = 2$). The numerical study for generalized situations confirms our analytical result using the two-level model.

DOI: 10.1103/PhysRevB.86.205305 PACS number(s): 72.25.Dc, 71.70.Ej, 73.23.−b, 85.75.−d

I. INTRODUCTION

The spin-orbit (SO) interaction in semiconductors has been studied extensively from viewpoints of its fundamental research and application to spin-based electronics, i.e., "spintronics."[1] For conduction electrons in direct-gap semiconductors, an external potential $U(\boldsymbol{r})$ results in the Rashba SO interaction[2,3]

$$H_{\mathrm{RSO}} = \frac{\lambda}{\hbar}\boldsymbol{\sigma}\cdot[\boldsymbol{p}\times\nabla U(\boldsymbol{r})], \tag{1}$$

where $\boldsymbol{p}$ is the momentum operator and $\boldsymbol{\sigma}$ is the Pauli matrix indicating the electron spin $\boldsymbol{s} = \boldsymbol{\sigma}/2$.[4] The coupling constant λ is markedly enhanced by the band effect, particularly in narrow-gap semiconductors such as InAs and InSb.[5,6] The bulk inversion symmetry is broken in compound semiconductors, which gives rise to another type of SO interaction, the Dresselhaus SO interaction.[7] It is given by

$$H_{\mathrm{DSO}} = \frac{\lambda'}{\hbar}\big[p_x\big(p_y^2 - p_z^2\big)\sigma_x + p_y\big(p_z^2 - p_x^2\big)\sigma_y + p_z\big(p_x^2 - p_y^2\big)\sigma_z\big]. \tag{2}$$

In the presence of SO interaction, the spin Hall effect (SHE) is one of the most important phenomena for the application to the spintronics. It produces a spin current traverse to an electric field applied by the bias voltage. There are two types of SHE. One is an intrinsic SHE, which is induced by the drift motion of carriers in the SO-split band structures. It creates a dissipationless spin current.[8–10] The other is an extrinsic SHE caused by the spin-dependent scattering of electrons by impurities.[11] Kato *et al.* observed the spin accumulation at sample edges traverse to the current,[12] which is ascribable to the extrinsic SHE with $U(\boldsymbol{r})$ being the screened Coulomb potential by charged impurities in Eq. (1).[13] The extrinsic SHE is usually understood semiclassically in terms of skew scattering and side-jump effect.

In our previous studies,[14,15] we theoretically examined the extrinsic SHE in semiconductor heterostructures due to the scattering by single artificial potential. The potential created by antidots, STM tips, and others is electrically tunable. We adopted the quantum mechanical scattering theory for this problem. When the potential is axially symmetric in two dimensions, $U(r)$ with $r = \sqrt{x^2 + y^2}$ in the xy plane, electrons feel the potential

$$U_{\mathrm{eff}} = U(r) + U_1(r)l_z\sigma_z \tag{3}$$

in the presence of Rashba SO interaction. $U_1(r) = -\lambda U'(r)/r$ has the same sign as $U(r)$ if $|U(r)|$ is a monotonically decreasing function of r and $\lambda > 0$. For electrons with $\sigma_z = 1$, $U_{\mathrm{eff}} = U(r) + U_1(r)l_z$ and as a result, the scattering for components of $l_z > 0$ ($l_z < 0$) is enhanced (suppressed) by the SO interaction. For electrons with $\sigma_z = -1$, the effect is opposite. This is the origin of the extrinsic SHE in two-dimensional electron systems. We showed that the SHE is significantly enhanced by the resonant scattering when $U(r)$ is attractive and properly tuned. We proposed a three-terminal spin filter including a single antidot.

In this study, we examine an enhancement of the "extrinsic SHE" by resonant tunneling through a quantum dot (QD) in multiterminal geometries. The QD is a well-known device showing a Coulomb oscillation when the electrostatic potential is tuned by a gate voltage.[16] The number of electrons is almost fixed by the Coulomb blockade between the current peaks of the oscillation. At the current peaks, the resonant tunneling takes place through discrete energy levels in the QD at low temperatures of $k_{\mathrm{B}}T \ll \Gamma$ with level broadening Γ due to the tunnel coupling to the leads. Recently, the SO interaction in QDs of narrow-gap semiconductors and related phenomena have been investigated intensively.[17–28] We consider a situation in which a QD with SO interaction is connected to N ($\geqslant 2$) external leads via tunnel barriers. We use the term SHE in the following meaning: When an unpolarized current is injected to the QD from a lead (lead S), polarized currents are ejected to the other leads [D1, . . . ,D($N-1$)]. In other words, the QD works as a spin filter. We assume that the SO interaction is present only in the QD and that the average of level spacing in the QD is comparable to the level broadening Γ ($\sim$1 meV), in accordance with experimental situations.[17] Thus, the transport takes place through single or a few energy levels in the QD around the Fermi level ε_{F} in the leads. The strength of SO interaction Δ_{SO} [absolute value of $\boldsymbol{h}_{\mathrm{SO}}$ in Eq. (6)] is approximately $0.1 \sim 0.2$ meV for InAs QDs (Refs. 18–21) and 0.23 meV for InSb QDs.[28]

Our purpose is to elucidate the mechanism of SHE at a QD with discrete energy levels. Consider an electron with spin up

or down injected to the QD from lead D1 (electric current flows from the QD to lead (D1). The SO interaction in the QD mixes a few energy levels around ε_F in a spin-dependent way [a rotation in the pseudospin space of the levels; see Eq. (8)], whereas the tunnel coupling to lead D2 mixes the levels differently in a spin-independent way. The interference between the mixings results in the spin-polarized electron going out to lead S. To simply clarify the spin-dependent transport processes, we neglect the electron-electron interaction. We focus on the current peaks of the Coulomb oscillation where the interaction is not qualitatively important.

First, we examine a two-level QD as a minimal model and present an analytical expression for the spin-dependent conductance. We assume a single conduction channel in each of the N leads. In the absence of magnetic field, we show that three or more leads ($N \geqslant 3$) are required to generate the spin-polarized current. We observe a large spin polarization by the resonant tunneling at the current peak when the spacing Δ between the two levels in the QD is smaller than Γ. Although the SHE at a QD seems quite different from the SHE by an impurity potential, the condition of $\Delta < \Gamma$ would correspond to the degeneracy for the virtual bound states with $\pm l_z$ [see Eq. (3)].[29] The preliminary results of this part in this paper were published in our previous paper.[30]

Second, we analyze the transport through the two-level QD in a weak magnetic field. The orbital magnetization is taken into account to the first order of magnetic field, whereas the Zeeman effect is neglected. We find the creation of spin-polarized current in a conventional geometry of two-terminal QD ($N = 2$) with finite magnetization b [see Eq. (7); $b \sim \hbar\omega_c$ with cyclotron frequency $\omega_c = |e|B/m^*$] and enhancement of the polarization when $|b|$ is comparable to the strength of the SO interaction Δ_{SO} (magnetic field of $B \sim 40$ mT). This is ascribable to the interference between the spin-dependent mixing of energy levels in the QD by the SO interaction and spin-independent one by the orbital magnetization.

Finally, our analytical results for the two-level QD are confirmed by numerical study on the QD with several energy levels. A QD with tunnel barriers to N leads is modeled on a two-dimensional tight-binding model. We observe spin-polarized currents for $N = 3$ ($N = 2$) in the absence (presence) of magnetic field. The spin polarization is markedly enhanced at the current peaks when a few energy levels are close to each other around ε_F. The polarized current is large enough to observe in experiments. We propose its detection by measuring the electric current through an "inverse SHE," if a QD is connected to a ferromagnetic lead.

We make some comments here. (i) Previous theoretical papers[31–34] concerned the spin-current generation in a mesoscopic region, or an open QD with no tunnel barriers, in which many energy levels in the QD participate in the transport. Since we are interested in the resonant tunneling through one or two discrete levels in the QD, our situation is different from that in the papers. (ii) This work indicates a QD spin filter in multiterminal (two-terminal) geometries without (with) magnetic field although we emphasize the fundamental aspect of the mechanism for the SHE at a QD. Note that our spin filter works only at low temperatures since the SHE stems from the coherent transport processes through the QD. Other spin filters were proposed using semiconductor nanostructures with SO interaction, e.g., three- or four-terminal devices related to the SHE,[14,15,35–40] a triple-barrier tunnel diode,[41] quantum point contact,[42,43] and a three-terminal device for the Stern-Gerlach experiment using a nonuniform SO interaction.[44] (iii) We do not consider the electron-electron interaction in this paper, focusing on the current peaks of the Coulomb oscillation. In the Coulomb blockade regimes between the current peaks, the electron-electron interaction plays a crucial role. We examined the many-body resonance induced by the Kondo effect in the blockade regime with spin-1/2 in the multiterminal QD. We showed the generation of largely polarized current in the presence of the SU(4) Kondo effect when the level spacing is less than the Kondo temperature.[30] We also mention that an enhancement of SHE by the resonant scattering or Kondo resonance was examined for metallic systems with magnetic impurities.[45–47]

The organization of this paper is as follows. In Sec. II, we explain a model of two-level QD connected to N external leads. Section III presents the analytical expressions for the spin-dependent conductance using the two-level model. In Sec. IV, we study a generalized situation in which a QD with many energy levels is connected to N leads through tunnel barriers. We make a two-dimensional tight-binding model to describe the situation and perform a numerical study. The last section (Sec. V) is devoted to the conclusions and discussion.

II. MODEL OF TWO-LEVEL QUANTUM DOT

In this section, we explain our model depicted in Fig. 1(a), in which a two-level QD is connected to N external leads. We start from a QD with SO interaction and magnetic field $\boldsymbol{B}$ in general. The electronic state in the QD is described by the Hamiltonian

$$H_{\rm dot}^{(0)} = \frac{(\boldsymbol{p} - e\boldsymbol{A})^2}{2m^*} + U(\boldsymbol{r}) + H_{\rm SO}(\boldsymbol{B}) \tag{4}$$

$$\simeq \frac{\boldsymbol{p}^2}{2m^*} + U(\boldsymbol{r}) + \frac{|e|\hbar}{2m^*}\boldsymbol{B}\cdot\boldsymbol{l} + H_{\rm SO}, \tag{5}$$

where $U(\boldsymbol{r})$ is the confining potential of the QD, m^* is the effective mass of conduction electrons ($m^*/m_0 = 0.024$ in InAs with m_0 being the electron mass in the vacuum), and $\boldsymbol{A} = (\boldsymbol{B}\times\boldsymbol{r})/2$ is the vector potential. Assuming a weak magnetic field, we neglect the term of $\boldsymbol{A}^2$ and Zeeman effect. For the SO interaction, $H_{\rm SO}$ can be the Rashba and/or Dresselhaus interactions in Eqs. (1) and (2). Although $\boldsymbol{p}$ in $H_{\rm SO}$ should be replaced by $(\boldsymbol{p} - e\boldsymbol{A})$ in the presence of magnetic field, the terms of $\boldsymbol{A}$ in $H_{\rm SO}(\boldsymbol{B})$ can be disregarded in the case of weak magnetic field (see Appendix A).

The eigenenergies of $\boldsymbol{p}^2/(2m^*) + U(\boldsymbol{r})$ form a set of discrete energy levels $\{\varepsilon_i\}$. We examine the situation in which two energy levels ε_1 and ε_2 are relevant to the transport. The other levels are located so far from the two levels that the mixing by $H_{\rm SO}$ or $|e|\hbar\boldsymbol{B}\cdot\boldsymbol{l}/(2m^*)$ can be neglected.

The wave functions of the states $\langle\boldsymbol{r}|1\rangle$ and $\langle\boldsymbol{r}|2\rangle$ can be real since they are eigenstates of real operator $\boldsymbol{p}^2/(2m^*) + U(\boldsymbol{r})$. Since the orbital part in $H_{\rm SO}$ is a pure imaginary operator, it has off-diagonal elements only:

$$\langle 2|H_{\rm SO}|1\rangle = \mathrm{i}\boldsymbol{h}_{\rm SO}\cdot\boldsymbol{\sigma}/2 \tag{6}$$

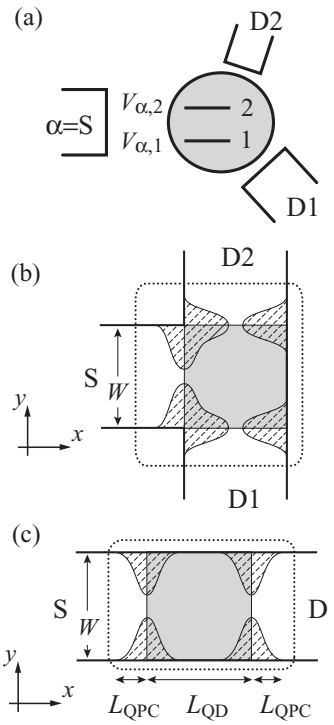

FIG. 1. Models for a quantum dot (QD) connected to N ($\geqslant 2$) leads. When an unpolarized current is injected to the QD from lead S, polarized currents are ejected to leads D1 to D($N-1$). (a) A QD with two energy levels. The tunnel coupling between level j (=1,2) in the QD and lead α is denoted by $V_{\alpha,j}$. (b) A QD (shaded square region of $W \times W$ in area) connected to three leads (quantum wires of W in width) via quantum point contacts. (c) A QD connected to two leads via quantum point contacts in the presence of magnetic field. Models in (b) and (c) are represented on a tight-binding model by discretizing the two-dimensional space (xy plane).

with $\boldsymbol{h}_{\rm SO} = \boldsymbol{h}_{\rm RSO} + \boldsymbol{h}_{\rm DSO}$. $i\boldsymbol{h}_{\rm RSO} = (2\lambda/\hbar)\langle 2|(\boldsymbol{p} \times \nabla U)|1\rangle$ in the case of Rashba interaction, whereas $ih_{{\rm DSO},x} = (2\lambda'/\hbar)\langle 2|p_x(p_y^2 - p_z^2)|1\rangle$, etc., in the case of Dresselhaus interaction. For the same reason, $\langle 1|\boldsymbol{B}\cdot\boldsymbol{l}|1\rangle = \langle 2|\boldsymbol{B}\cdot\boldsymbol{l}|2\rangle = 0$ and

$$\frac{|e|\hbar}{m^*}\langle 2|\boldsymbol{B}\cdot\boldsymbol{l}|1\rangle = ib/2. \tag{7}$$

We estimate the value of $|b|$ to be $|e|\hbar B/m^* = \hbar\omega_{\rm c}$, where $\omega_{\rm c} = |e|B/m^*$ is the cyclotron frequency. When $\hbar\omega_{\rm c} = 0.2$ meV ($\simeq\Delta_{\rm SO}$), the corresponding magnetic field is $B = 40$ mT in the case of InAs. If the quantization axis of spin is taken in the direction of $\boldsymbol{h}_{\rm SO}$, the Hamiltonian in the QD reads as

$$H_{\rm dot} = \sum_{\sigma=\pm}(d_{1,\sigma}^\dagger, d_{2,\sigma}^\dagger)\left(\bar{\varepsilon} - \frac{\Delta}{2}\tau_z + \frac{b+\sigma\Delta_{\rm SO}}{2}\tau_y\right)\begin{pmatrix} d_{1,\sigma} \\ d_{2,\sigma}\end{pmatrix}, \tag{8}$$

where $d_{j,\sigma}^\dagger$ and $d_{j,\sigma}$ are the creation and annihilation operators of an electron with orbital j and spin σ, respectively. $\bar{\varepsilon} = (\varepsilon_1 + \varepsilon_2)/2$, $\Delta = \varepsilon_2 - \varepsilon_1$, and $\Delta_{\rm SO} = |\boldsymbol{h}_{\rm SO}|$. The Pauli matrices τ_y and τ_z are introduced for the pseudospin representing levels 1 or 2 in the QD. Note that the Hamiltonian in Eq. (8) yields the energy levels of $\bar{\varepsilon} \pm \sqrt{\Delta^2 + (b+\sigma\Delta_{\rm SO})^2}/2$ for $\sigma = +$ or $-$ in an isolated QD; the Kramers degeneracy holds only with $b = 0$. Although the average of level spacing in a QD is assumed to be $\delta \sim 1$ meV, the spacing Δ between a specific pair of levels fluctuates around δ. Δ is fixed while the electrostatic potential, and hence the mean energy level $\bar{\varepsilon}$, is changed by tuning the gate voltage.

The state $|j\rangle$ in the QD is connected to lead α by tunnel coupling $V_{\alpha,j}$ ($j = 1,2$), which is real. The tunnel Hamiltonian is

$$\begin{aligned} H_{\rm T} &= \sum_{\alpha}^{\rm (leads)}\sum_{k,\sigma}\sum_{j=1}^{2}(V_{\alpha,j}d_{j,\sigma}^\dagger a_{\alpha k,\sigma} + {\rm H.c.}) \\ &= \sum_{\alpha}^{\rm (leads)}\sum_{k,\sigma} V_\alpha[(e_{\alpha,1}d_{1,\sigma}^\dagger + e_{\alpha,2}d_{2,\sigma}^\dagger)a_{\alpha k,\sigma} + {\rm H.c.}], \end{aligned} \tag{9}$$

where $a_{\alpha k,\sigma}$ annihilates an electron with state k and spin σ in lead α. $V_\alpha = \sqrt{(V_{\alpha,1})^2 + (V_{\alpha,2})^2}$ and $e_{\alpha,j} = V_{\alpha,j}/V_\alpha$. We introduce a unit vector $\boldsymbol{e}_\alpha = (e_{\alpha,1}, e_{\alpha,2})^{\rm T}$. V_α is controllable by electrically tuning the tunnel barrier, whereas $\boldsymbol{e}_\alpha$ is determined by the wave functions $\langle \boldsymbol{r}|1\rangle$ and $\langle \boldsymbol{r}|2\rangle$ in the QD and hardly controllable for a given current peak. It should be mentioned that $\{\boldsymbol{e}_\alpha\}$ and Δ vary from peak to peak in the Coulomb oscillation. We can choose a peak with appropriate parameters for the SHE in experiments.

We assume a single channel of conduction electrons in the leads. The total Hamiltonian is

$$H = \sum_{\alpha}^{\rm (leads)}\sum_{k,\sigma}\varepsilon_k c_{\alpha k,\sigma}^\dagger c_{\alpha k,\sigma} + H_{\rm dot} + H_{\rm T}. \tag{10}$$

The strength of tunnel coupling to lead α is characterized by the level broadening $\Gamma_\alpha = \pi\nu_\alpha(V_\alpha)^2$, where ν_α is the density of states in the lead. We also introduce a matrix of $\hat{\Gamma} = \sum_\alpha \hat{\Gamma}_\alpha$ with

$$\hat{\Gamma}_\alpha = \Gamma_\alpha\begin{pmatrix} (e_{\alpha,1})^2 & e_{\alpha,1}e_{\alpha,2} \\ e_{\alpha,1}e_{\alpha,2} & (e_{\alpha,2})^2\end{pmatrix}. \tag{11}$$

An unpolarized current is injected into the QD from a source lead ($\alpha = {\rm S}$) and output to other leads [Dn; $n = 1, \ldots, (N-1)$]. The electrochemical potential for electrons in lead S is lower than that in the other leads by $|e|V_{\rm bias}$. The transport through a QD in the multiterminal geometry can be formulated following the paper by Meir and Wingreen,[48] just as in the two-terminal geometry. The current with spin $\sigma = \pm$ from lead α to the QD is written as

$$I_{\alpha,\sigma} = \frac{ie}{\pi\hbar}\int d\varepsilon\, {\rm Tr}\{\hat{\Gamma}_\alpha[f_\alpha(\varepsilon)(\hat{G}_\sigma^{\rm r} - \hat{G}_\sigma^{\rm a}) + \hat{G}_\sigma^<]\}, \tag{12}$$

where $\hat{G}_\sigma^{\rm r}$, $\hat{G}_\sigma^{\rm a}$, and $\hat{G}_\sigma^<$ are the retarded, advanced, and lesser Green's functions in the QD, respectively, in 2×2 matrix form in the pseudospin space. $f_\alpha(\varepsilon)$ is the Fermi distribution function in lead α.

Although the current formula in Eq. (12) is applicable in the presence of electron-electron interaction in the QD, it is simplified in its absence. Then, $\hat{G}_\sigma^{\rm r} - \hat{G}_\sigma^{\rm a} = -2i\hat{G}_\sigma^{\rm r}\hat{\Gamma}\hat{G}_\sigma^{\rm a}$ and $\hat{G}_\sigma^< = 2i\hat{G}_\sigma^{\rm r}(\sum_\alpha \hat{\Gamma}_\alpha f_\alpha)\hat{G}_\sigma^{\rm a}$. The substitution of these relations

into Eq. (12) yields

$$I_{\mathrm{D}n,\sigma} = \frac{4e}{h}\int d\varepsilon[f_{\mathrm{D}}(\varepsilon) - f_{\mathrm{S}}(\varepsilon)]\mathrm{Tr}\big(\hat{G}^{\mathrm{a}}_{\sigma}\hat{\Gamma}_{\mathrm{D}n}\hat{G}^{\mathrm{r}}_{\sigma}\hat{\Gamma}_{\mathrm{S}}\big),$$

where $f_{\mathrm{D}n}(\varepsilon) \equiv f_{\mathrm{D}}(\varepsilon)$. At $T = 0$, the conductance into lead Dn with spin σ is given by

$$G_{n,\sigma} = -\frac{dI_{\mathrm{D}n,\sigma}}{dV_{\mathrm{bias}}}\bigg|_{V_{\mathrm{bias}}=0} = \frac{4e^2}{h}\mathrm{Tr}\big[\hat{G}^{\mathrm{a}}_{\sigma}(\varepsilon_{\mathrm{F}})\hat{\Gamma}_{\mathrm{D}n}\hat{G}^{\mathrm{r}}_{\sigma}(\varepsilon_{\mathrm{F}})\hat{\Gamma}_{\mathrm{S}}\big], \tag{13}$$

where the QD Green's function is

$$\hat{G}^{\mathrm{r}}_{\pm}(\varepsilon) = \left[\begin{pmatrix} \varepsilon - \varepsilon_{\mathrm{d}} + \frac{\Delta}{2} & \mathrm{i}\frac{b\pm\Delta_{\mathrm{SO}}}{2} \\ -\mathrm{i}\frac{b\pm\Delta_{\mathrm{SO}}}{2} & \varepsilon - \varepsilon_{\mathrm{d}} - \frac{\Delta}{2} \end{pmatrix} + \mathrm{i}\hat{\Gamma}\right]^{-1}. \tag{14}$$

III. ANALYTICAL RESULTS

We analyze the model of two-level QD, introduced in the previous section. We show analytical expressions for the spin-dependent conductance in the absence and presence of magnetic field, respectively.

A. In absence of magnetic field

We begin with the case of $b = 0$, or in the absence of magnetic field. From Eqs. (13) and (14), we obtain

$$G_{n,\sigma} = \frac{e^2}{h}\frac{4\Gamma_{\mathrm{S}}\Gamma_{\mathrm{D}n}}{|D|^2}\big[g^{(1)}_n + g^{(2)}_{n,\sigma}\big], \tag{15}$$

$$g^{(1)}_n = \left[\left(\varepsilon_{\mathrm{F}} - \bar{\varepsilon} - \frac{\Delta}{2}\right)e_{\mathrm{D}n,1}e_{\mathrm{S},1} + \left(\varepsilon_{\mathrm{F}} - \bar{\varepsilon} + \frac{\Delta}{2}\right)e_{\mathrm{D}n,2}e_{\mathrm{S},2}\right]^2, \tag{16}$$

$$g^{(2)}_{n,\pm} = \left[\pm\frac{\Delta_{\mathrm{SO}}}{2}(\boldsymbol{e}_{\mathrm{S}}\times\boldsymbol{e}_{\mathrm{D}n})_z + \sum_{\alpha}^{(\mathrm{leads})}\Gamma_{\alpha}(\boldsymbol{e}_{\mathrm{D}n}\times\boldsymbol{e}_{\alpha})_z(\boldsymbol{e}_{\mathrm{S}}\times\boldsymbol{e}_{\alpha})_z\right]^2, \tag{17}$$

where D is the determinant of $[\hat{G}^{\mathrm{r}}_{\sigma}(\varepsilon_{\mathrm{F}})]^{-1}$ in Eq. (14), which is independent of σ. $(\boldsymbol{a}\times\boldsymbol{b})_z = a_1b_2 - a_2b_1$.

Let us consider two simple cases. (1) When $\Delta \gg \Gamma_{\alpha}$ and Δ_{SO}, $G_{n,\sigma}$ consists of two Lorentzian peaks as a function of $\bar{\varepsilon}$, reflecting the resonant tunneling through one of the energy levels $\varepsilon_{1,2} = \bar{\varepsilon} \mp \Delta/2$:

$$G_{n,\sigma} \approx \frac{4e^2}{h}\Gamma_{\mathrm{S}}\Gamma_{\mathrm{D}n}\sum_{j=1,2}\frac{(e_{\mathrm{D}n,j}e_{\mathrm{S},j})^2}{(\varepsilon_j - \varepsilon_{\mathrm{F}})^2 + (\Gamma_{jj})^2}. \tag{18}$$

Here, $\Gamma_{jj} = \sum_{\alpha}\pi\nu_{\alpha}(V_{\alpha,j})^2$ is the broadening of level j (jj component of matrix $\hat{\Gamma}$). In this case, the spin-polarized current [$\propto (G_{n,+} - G_{n,-})$] is very small. Δ should be comparable to or smaller than the level broadening to observe a considerable spin current. (2) In a two-terminal QD ($N = 2$), the term of $\sum_{\alpha}$ vanishes in $g^{(2)}_{n,\pm}$. Since $g^{(2)}_{n,+} = g^{(2)}_{n,-}$, no spin-polarized current is generated.[49] Three or more leads are required to generate a spin-polarized current, as pointed out by other groups.[31,33,50]

We examine $G_{1,\pm}$ in the three-terminal system ($N = 3$) in the rest of this section. Then, $g^{(2)}_{1,\pm} = [\pm(\Delta_{\mathrm{SO}}/2)(\boldsymbol{e}_{\mathrm{S}}\times\boldsymbol{e}_{\mathrm{D}1})_z + \Gamma_{\mathrm{D}2}(\boldsymbol{e}_{\mathrm{D}1}\times\boldsymbol{e}_{\mathrm{D}2})_z(\boldsymbol{e}_{\mathrm{S}}\times\boldsymbol{e}_{\mathrm{D}2})_z]^2$. We exclude specific situations in which two out of $\boldsymbol{e}_{\mathrm{S}}$, $\boldsymbol{e}_{\mathrm{D}1}$, and $\boldsymbol{e}_{\mathrm{D}2}$ are parallel to each other. The conditions for a largely spin-polarized current are as follows: (i) $\Delta \lesssim$ (level broadening), as mentioned above. Two levels in the QD should participate in the transport. (ii) The Fermi level in the leads is close to the energy levels in the QD, $\varepsilon_{\mathrm{F}} \approx \bar{\varepsilon}$ (resonant condition). (iii) The level broadening by the tunnel coupling to lead D2, $\Gamma_{\mathrm{D}2}$, is comparable to the strength of SO interaction Δ_{SO}.

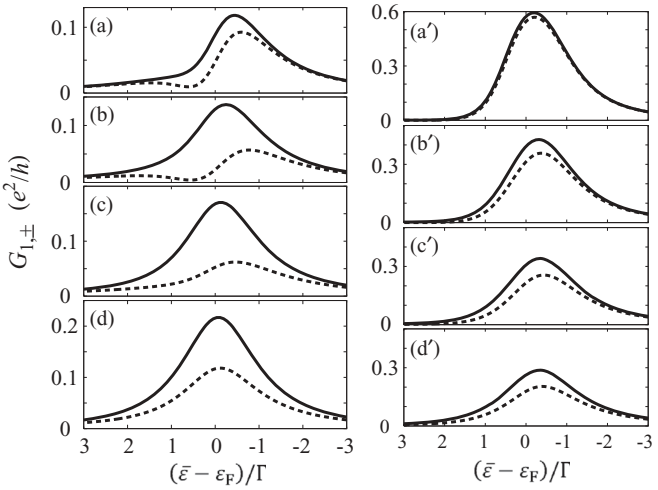

FIG. 2. Spin-dependent conductance $G_{1,\pm}$ in the model of two-level quantum dot in the three-terminal geometry, as a function of mean energy level $\bar{\varepsilon} = (\varepsilon_1 + \varepsilon_2)/2$. No magnetic field is applied. Solid (broken) lines indicate the conductance $G_{1,+}$ ($G_{1,-}$) for spin $\sigma = +1$ (-1) in the direction of $\boldsymbol{h}_{\mathrm{SO}}$ (see Sec. II). The level spacing in the quantum dot is $\Delta = \varepsilon_2 - \varepsilon_1 = 0.2\Gamma$ (left panels) and Γ (right panels). The level broadening by the tunnel coupling to leads S and D1 is $\Gamma_{\mathrm{S}} = \Gamma_{\mathrm{D}1} \equiv \Gamma$ ($e_{\mathrm{S},1}/e_{\mathrm{S},2} = 1$, $e_{\mathrm{D}1,1}/e_{\mathrm{D}1,2} = -2/3$), whereas that to lead D2 is (a) $\Gamma_{\mathrm{D}2} = 0.1\Gamma$, (b) 0.5Γ, (c) Γ, and (d) 2Γ ($e_{\mathrm{D}2,1}/e_{\mathrm{D}2,2} = 2$). The strength of spin-orbit interaction is fixed at $\Delta_{\mathrm{SO}} = 0.2\Gamma$.

Figures 2 and 4 show two typical results of the conductance $G_{1,\pm}$ as a function of $\bar{\varepsilon}$. In $g^{(1)}_1$, $e_{\mathrm{D}1,1}e_{\mathrm{S},1}$ and $e_{\mathrm{D}1,2}e_{\mathrm{S},2}$ have different (same) signs in Fig. 2 (Fig. 4). Therefore, $g^{(1)}_1 = 0$ has no solution (a solution) in $-\Delta/2 < \bar{\varepsilon} - \varepsilon_{\mathrm{F}} < \Delta/2$. In Fig. 2, the conductance shows a single peak. We set $\Gamma_{\mathrm{S}} = \Gamma_{\mathrm{D}1} \equiv \Gamma$ and change $\Gamma_{\mathrm{D}2}$ from Fig. 2(a) 0.1Γ to Fig. 2(d) 2Γ. When $\Delta = 0.2\Gamma$ (left panels), we observe a large spin polarization around the current peak, which clearly indicates an enhancement of the SHE by the resonant tunneling [conditions (i) and (ii)]. With increasing $\Gamma_{\mathrm{D}2}$, the spin current increases first, takes a maximum in Fig. 2(c), and then decreases [condition (iii)]. This means that the SHE is tunable by changing the tunnel coupling. When $\Delta = \Gamma$ (right panels), the SHE is less effective; spin polarization of $P = (G_{1,+} - G_{1,-})/(G_{1,+} + G_{1,-})$ around the current peak is smaller than in the case of $\Delta = 0.2\Gamma$. However, a value of spin-polarized conductance $G_{n,+} - G_{n,-}$ is still large, as depicted in Fig. 3.

In Fig. 4, the conductance $G_{1,\pm}$ shows a dip at $\bar{\varepsilon} \approx \varepsilon_{\mathrm{F}}$ for small $\Gamma_{\mathrm{D}2}$. The conductance dip is caused by the destructive interference between propagating waves through two orbitals in the QD. In the two-terminal QD without SO interaction ($\Gamma_{\mathrm{D}2} = \Delta_{\mathrm{SO}} = 0$), the conductance $G_{1,\sigma} \propto g^{(1)}_1$

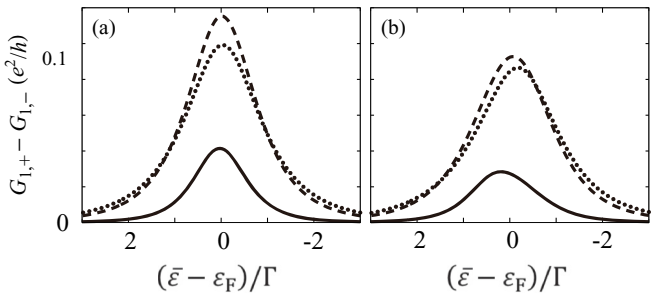

FIG. 3. Spin-polarized conductance $G_{1,+} - G_{1,-}$ in the model of two-level quantum dot in the three-terminal geometry, as a function of $\bar{\varepsilon}$. The level spacing in the quantum dot is (a) $\Delta = \varepsilon_2 - \varepsilon_1 = 0.2\Gamma$ and (b) Γ. $\Gamma_{D2} = 0.1\Gamma$ (solid line), Γ (broken line), and 2Γ (dotted line). The other parameters are the same as in Fig. 2.

would completely vanish at the dip, where the "phase lapse" of the transmission phase takes place.[51] As seen in Fig. 4, the conductance dip changes to a peak with increasing Γ_{D2} in the three-terminal QD. The SO interaction makes a large difference between $G_{1,+}$ and $G_{1,-}$ around the dip or peak, similarly to the case in Fig. 2. The spin-polarized conductance $G_{1,+} - G_{1,-}$ shows a large peak there, as seen in the inset in Fig. 4. In Fig. 4(a) with $\Gamma_{D2} = 0.1\Gamma$, we find that the spin polarization of $P = (G_{1,+} - G_{1,-})/(G_{1,+} + G_{1,-})$ is close to unity around the dip since $G_{1,-}$ is almost zero.

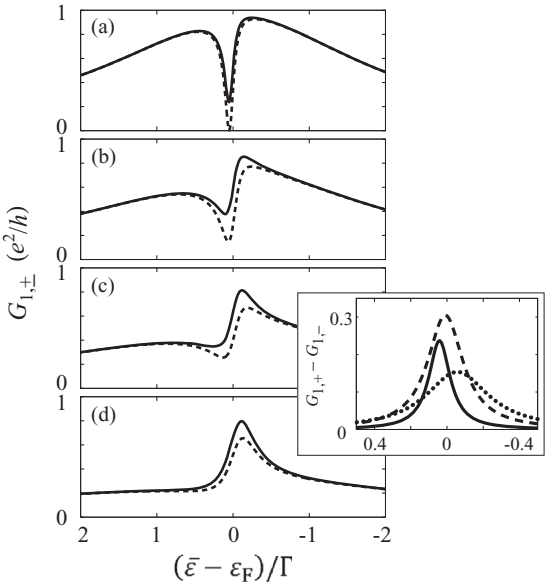

FIG. 4. Spin-dependent conductance $G_{1,\pm}$ in the model of two-level quantum dot in the three-terminal geometry, as a function of mean energy level $\bar{\varepsilon} = (\varepsilon_1 + \varepsilon_2)/2$. No magnetic field is applied. Solid (broken) lines indicate the conductance $G_{1,+}$ ($G_{1,-}$) for spin $\sigma = +1$ (-1) in the direction of $\boldsymbol{h}_{SO}$ (see Sec. II). The level spacing in the quantum dot is $\Delta = \varepsilon_2 - \varepsilon_1 = 0.5\Gamma$. The level broadening by the tunnel coupling to leads S and D1 is $\Gamma_S = \Gamma_{D1} \equiv \Gamma$ ($e_{S,1}/e_{S,2} = 1$, $e_{D1,1}/e_{D1,2} = 2/3$), whereas that to lead D2 is (a) $\Gamma_{D2} = 0.1\Gamma$, (b) 0.5Γ, (c) Γ, and (d) 2Γ ($e_{D2,1}/e_{D2,2} = 2$). The strength of spin-orbit interaction is fixed at $\Delta_{SO} = 0.2\Gamma$. Inset: Spin-polarized conductance $(G_+ - G_-)$ in units of e^2/h, as a function of $\bar{\varepsilon}$. $\Gamma_{D2} = 0.1\Gamma$ (solid line), 0.5Γ (broken line), and 2Γ (dotted line).

B. In presence of magnetic field

Now, we discuss the case with magnetic field: $b \neq 0$. The conductance into lead Dn with spin σ is

$$G_{n,\sigma} = \frac{e^2}{h} \frac{4\Gamma_S \Gamma_{Dn}}{|D_\sigma|^2} \left[g_n^{(1)} + g_{n,\sigma}^{(2)} \right], \tag{19}$$

where $g_n^{(1)}$ is the same as that in Eq. (16), whereas

$$g_{n,\pm}^{(2)} = \left[\frac{b \pm \Delta_{SO}}{2} (\boldsymbol{e}_S \times \boldsymbol{e}_{Dn})_z + \sum_{\alpha}^{(\text{leads})} \Gamma_\alpha (\boldsymbol{e}_{Dn} \times \boldsymbol{e}_\alpha)_z (\boldsymbol{e}_S \times \boldsymbol{e}_\alpha)_z \right]^2. \tag{20}$$

The determinant of $[\hat{G}_\sigma^r(\varepsilon_F)]^{-1}$, D_σ, depends on σ in this case.

In contrast to the case of $b = 0$, we observe the spin-dependent transport in a conventional geometry of two-terminal QD ($N = 2$). Then, $g_{1,\pm}^{(2)} = (b \pm \Delta_{SO})^2 (\boldsymbol{e}_S \times \boldsymbol{e}_{D1})_z^2/4$. We expect a large spin polarization when (iii′) b and Δ_{SO} are comparable to each other, besides conditions (i) and (ii) in the previous section are satisfied.

We focus on the two-terminal QD ($N = 2$) in this section. Figures 5 and 7 exhibit the spin-dependent conductance $G_{1,\pm}$ as a function of $\bar{\varepsilon}$. $e_{D1,1}e_{S,1}$ and $e_{D1,2}e_{S,2}$ have different (same) signs in Fig. 5 (Fig. 7). We set $\Gamma_S = \Gamma_{D1} \equiv \Gamma$, whereas the orbital magnetization is gradually increased from (a) to (d) in Fig. 5, or from (a) to (c) in Fig. 7. In Fig. 5, the level spacing in the QD is $\Delta = 0.2\Gamma$ in the left panels and $\Delta = \Gamma$ in the right panels. In the absence of magnetic field ($b = 0$), we do not observe the spin-polarized current in the two-terminal

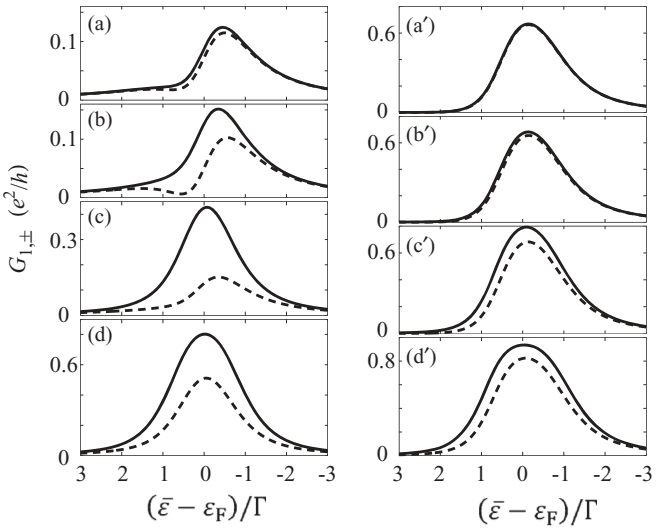

FIG. 5. Spin-dependent conductance $G_{1,\pm}$ in the model of two-level quantum dot in the two-terminal geometry, as a function of mean energy level $\bar{\varepsilon} = (\varepsilon_1 + \varepsilon_2)/2$, in the presence of magnetic field. Solid (broken) lines indicate the conductance $G_{1,+}$ ($G_{1,-}$) for spin $\sigma = +1$ (-1) in the direction of $\boldsymbol{h}_{SO}$ (see Sec. II). The level spacing in the quantum dot is $\Delta = \varepsilon_2 - \varepsilon_1 = 0.2\Gamma$ (left panels) and Γ (right panels). The level broadening by the tunnel coupling to leads S and D1 is $\Gamma_S = \Gamma_{D1} \equiv \Gamma$ ($e_{S,1}/e_{S,2} = 1$, $e_{D1,1}/e_{D1,2} = -2/3$). The orbital magnetization is (a) $b = 0.02\Gamma$, (b) 0.1Γ, (c) 0.5Γ, and (d) Γ. The strength of spin-orbit interaction is fixed at $\Delta_{SO} = 0.2\Gamma$.

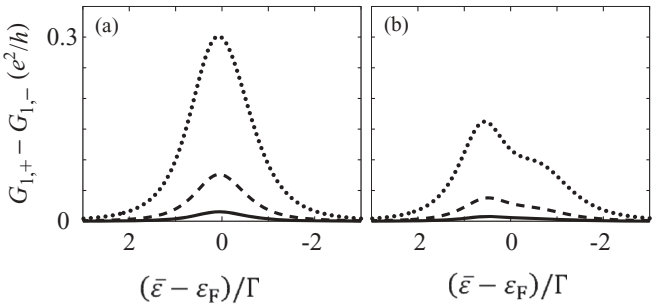

FIG. 6. Spin-polarized conductance $G_{1,+} - G_{1,-}$ in the model of two-level quantum dot in the two-terminal geometry, as a function of $\bar{\varepsilon}$, in the presence of magnetic field. The level spacing in the quantum dot is (a) $\Delta = \varepsilon_2 - \varepsilon_1 = 0.2\Gamma$ and (b) Γ. The orbital magnetization b is $b = 0.02\Gamma$ (solid line), 0.1Γ (broken line), and 0.5Γ (dotted line). The other parameters are the same as in Fig. 5.

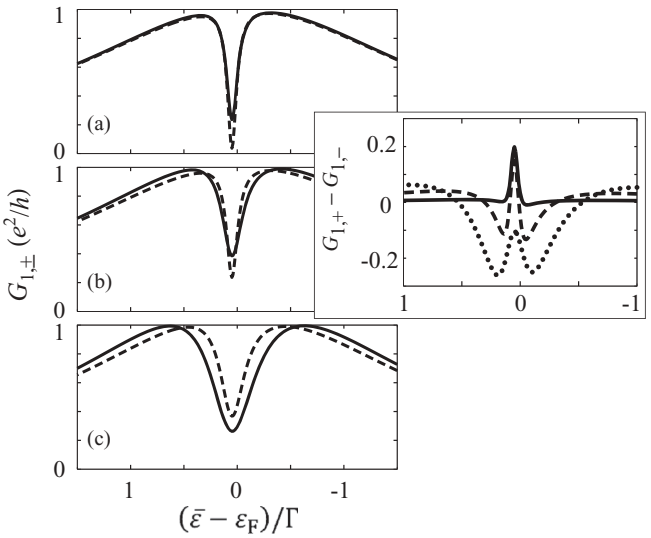

FIG. 7. Spin-dependent conductance $G_{1,\pm}$ in the model of two-level quantum dot in the two-terminal geometry, as a function of mean energy level $\bar{\varepsilon} = (\varepsilon_1 + \varepsilon_2)/2$, in the presence of magnetic field. Solid (broken) lines indicate the conductance $G_{1,+}$ ($G_{1,-}$) for spin $\sigma = +1$ (-1) in the direction of $\boldsymbol{h}_{SO}$ (see Sec. II). The level spacing in the quantum dot is $\Delta = \varepsilon_2 - \varepsilon_1 = 0.5\Gamma$. The level broadening by the tunnel coupling to leads S and D1 is $\Gamma_S = \Gamma_{D1} \equiv \Gamma$ ($e_{S,1}/e_{S,2} = 1$, $e_{D1,1}/e_{D1,2} = 2/3$). The orbital magnetization is (a) $b = 0.1\Gamma$, (b) 0.5Γ, and (c) Γ. The strength of spin-orbit interaction is fixed at $\Delta_{SO} = 0.2\Gamma$. Inset: Spin-polarized conductance ($G_+ - G_-$) in units of e^2/h, as a function of $\bar{\varepsilon}$. $b = 0.1\Gamma$ (solid line), 0.5Γ (broken line), and Γ (dotted line).

geometry, as discussed in the previous section. With an increase in b, the difference between $G_{1,+}$ and $G_{1,-}$ increases, becomes maximal at $b \sim \Delta_{SO}$, and decreases [condition (iii′)]. The SHE is more prominent for $\Delta = 0.2\Gamma$ than for $\Delta = \Gamma$; the polarization P is larger in the former. Figure 6 shows the spin-polarized conductance $G_{1,+} - G_{1,-}$ as a function of $\bar{\varepsilon}$. We observe a large value even in the case of $\Delta = \Gamma$ if both the magnetic field and $\bar{\varepsilon}$ are properly tuned.

In Fig. 7, we observe a dip of conductance at $\bar{\varepsilon} \approx \varepsilon_F$. Around the dip, the spin-polarized current is largely enhanced as shown in the inset. In Fig. 7(a), with $b = 0.1\Gamma$, the spin polarization of $P = (G_{1,+} - G_{1,-})/(G_{1,+} + G_{1,-})$ is close to unity because $G_{1,-}$ almost vanishes.

IV. NUMERICAL STUDY

In the previous section, we have presented the analytical expressions for the spin-dependent conductance for the model of two-level QD. We have illustrated the generation of spin-polarized current in three- and two-terminal geometries in the absence and presence of magnetic field, respectively. In this section, we perform numerical studies for the QD with many energy levels to confirm our analytical results. A QD with tunnel barriers to N leads ($N = 2,3$) in Figs. 1(b) and 1(c) is modeled on the tight-binding model in the xy plane.

A. Model

In Figs. 1(b) and 1(c), N leads connect to a QD via tunnel barriers. The N leads are represented by quantum wires of width W with hard-wall potential at the edges. The electrostatic potential in the QD (shaded square region of $W \times W$) is changed by eV_g. The tunnel barriers are described by quantum point contacts (QPCs). Along a quantum wire in the x direction, the QPC is described by the potential[52]

$$U(x,y;U_0) = \left\{ \frac{U_0}{2}\left[1 + \cos\left(\frac{\pi x}{L_{QPC}}\right)\right] + \varepsilon_F \sum_{\pm} \left(\frac{y - y_{\pm}(x)}{W_{QPC}}\right)^2 \theta(y^2 - y_{\pm}(x)^2) \right\} \quad (21)$$

at $-L_{QPC} < x < L_{QPC}$, where

$$y_{\pm}(x) = \pm\frac{W}{4}\left[1 - \cos\left(\frac{\pi x}{L_{QPC}}\right)\right] \quad (22)$$

and $\theta(t)$ is a step function [$\theta = 1$ for $t > 0$, $\theta = 0$ for $t < 0$]. U_0 is the potential height of the saddle point of QPC, whereas L_{QPC} and W_{QPC} characterize the thickness and width of the QPC, respectively. In the QD (shaded square region), the QPC potential is modified to $U(x,y;U_0 - eV_g) + eV_g$. In Fig. 1(b), we cut off the QPC potential at the diagonal lines of the square to avoid the overlap of two QPC potentials.

As for the SO interaction, we consider the Rashba interaction caused by the QPC potential in Eq. (21), that is,

$$H_{SO} = \frac{\lambda}{\hbar}\sigma_z\left[p_x\frac{\partial U}{\partial y} - p_y\frac{\partial U}{\partial x}\right]. \quad (23)$$

We choose the z direction for the spin axis ($\boldsymbol{h}_{SO} \parallel z$ direction). In the two-terminal geometry of Fig. 1(c), we consider a magnetic field perpendicular to the xy plane only in the region surrounded by dotted line. We adopt the vector potential of $\boldsymbol{A} = (-By,0,0)$ for the orbital magnetization and neglect the Zeeman effect. We discretize the two-dimensional space with QPC potentials and obtain the tight-binding model. We numerically evaluate the spin-dependent conductance, using the calculation method in Appendix B.

We consider the following situation. The width of quantum wires is $W = 100$ nm. The lattice constant of the tight-binding model is $a = W/30$ (number of sites is $M = 29$ in width of the wires). For the SO interaction, the dimensionless

coupling constant is $\tilde{\lambda} = \lambda/(2a^2) = 0.05$, which corresponds to $\lambda = 1.171\ \mathrm{nm}^2$ in InAs.[5] The Fermi wavelength and Fermi energy in the leads are fixed at $\lambda_F = W/3$ and $\varepsilon_F/t = 2 - 2\cos(2\pi a/\lambda_F) \simeq 0.382$, respectively. (There are six conduction channels in each lead. However, the single channel is effectively coupled to the QD owing to the QPC potential between the QD and the lead.) For the QPC potential, $L_{QPC} = W_{QPC} = \lambda_F$. $U_0 = 0.8\varepsilon_F$ at the connection to leads S and D1, whereas U_0 at the connection to lead D2 is changed from $U_0/\varepsilon_F = 1.1$ to 0.6 to tune the tunnel coupling Γ_{D2} in the three-terminal geometry of Fig. 1(b). In Fig. 1(c), the magnetic field is applied up to $\hbar\omega_c/\varepsilon_F = 30 \times 10^{-4}$, which corresponds to $B \simeq 34$ mT.

B. Numerical results

Figure 8 presents the spin-dependent conductance $G_{1,\sigma}$ in Fig. 1(b) of three-terminal QD, in the absence of magnetic field. $\sigma = \pm 1$ indicates the z component of electron spin. The conductance shows a peak structure as a function of electrostatic potential in the QD, eV_g, reflecting the resonant tunneling through discrete energy levels in the QD. Although this is similar to the Coulomb oscillation, the peak-peak distance is underestimated because we neglect the electron-electron interaction.

The average of the level spacing is larger than the level broadening in Fig. 8. Therefore, the difference between $G_{1,+}$ and $G_{1,-}$ is usually small. We observe a large spin-polarized conductance $G_{1,+} - G_{1,-}$ around some conductance peaks where a few levels should be close to each other around ε_F.

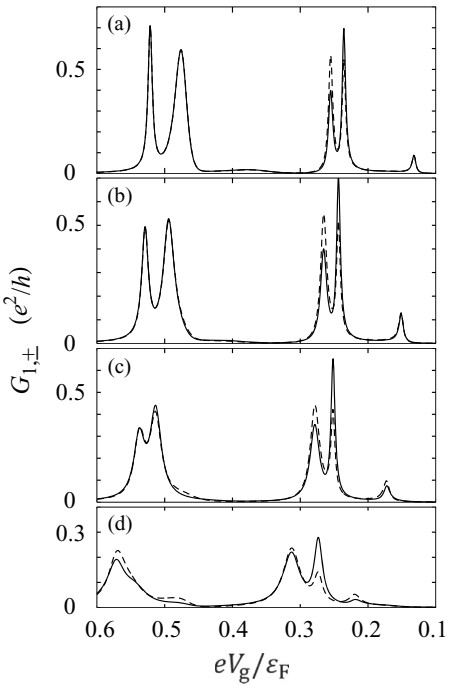

FIG. 8. Numerical results of spin-dependent conductance $G_{1,\pm}$ in model of Fig. 1(b), as a function of electrostatic potential in the quantum dot, eV_g. No magnetic field is applied. Solid (broken) lines indicate the conductance $G_{1,+}$ ($G_{1,-}$) for spin $\sigma = +1$ (-1) in the z direction. The height of QPC potential is $U_0 = 0.8\varepsilon_F$ at the connection to leads S and D1, whereas (a) $U_0/\varepsilon_F = 1.1$, (b) 0.9, (c) 0.8, and (d) 0.6 at the connection to lead D2.

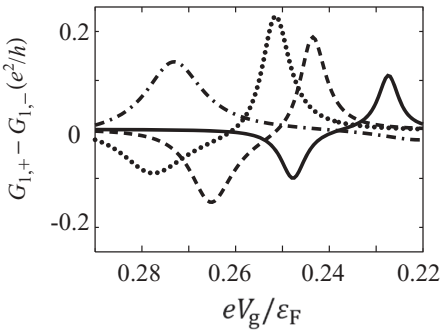

FIG. 9. Spin-polarized conductance $G_{1,+} - G_{1,-}$ as a function of eV_g in model of Fig. 1(b). The height of QPC potential at the connection to lead D2 is $U_0/\varepsilon_F = 1.1$ (solid line), 0.9 (broken line), 0.8 (dotted line), and 0.6 (dotted broken line). The other parameters are the same as in Fig. 8.

Look at the conductance around $eV_g/\varepsilon_F = 0.25$. With increasing the tunnel coupling to lead D2 by decreasing the height of QPC potential U_0, the spin-polarized conductance increases, becomes maximal, and decreases. This is in accordance with the analytical result in Sec. III A although it is hard to evaluate the level spacing and signs of tunnel coupling around ε_F. Figure 9 plots $G_{1,+} - G_{1,-}$ as a function of eV_g, which seems complicated probably due to the interference among three levels in the QD.

Figure 10 shows the spin-dependent conductance $G_{1,\sigma}$ in Fig. 1(c) of two-terminal QD, in the presence of magnetic field. A large spin-polarized conductance is obtained around $eV_g/\varepsilon_F = -0.21$. The difference of $G_{1,+} - G_{1,-}$ is changed with increasing magnetic field perpendicular to the QD. As shown in Fig. 11, the absolute value of spin-polarized

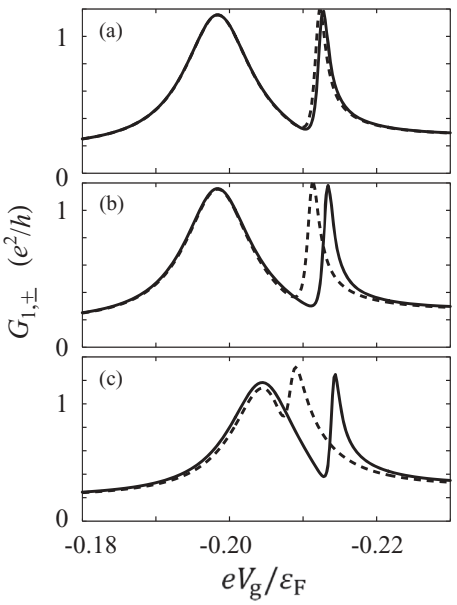

FIG. 10. Numerical results of spin-dependent conductance $G_{1,\pm}$ in model of Fig. 1(c), as a function of electrostatic potential in the quantum dot eV_g in the presence of magnetic field. Solid (broken) lines indicate the conductance $G_{1,+}$ ($G_{1,-}$) for spin $\sigma = +1$ (-1) in the z direction. The magnetic field is (a) $\hbar\omega_c/\varepsilon_F = 2 \times 10^{-4}$, (b) 10×10^{-4}, and (c) 30×10^{-4}.

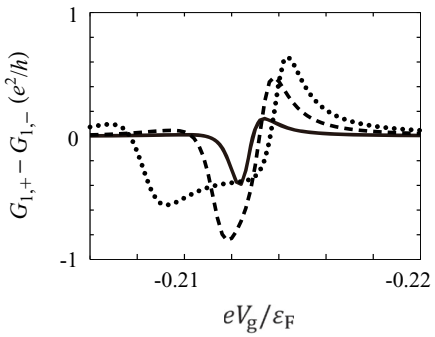

FIG. 11. Spin-polarized conductance $G_{1,+} - G_{1,-}$ as a function of eV_g in model of Fig. 1(c) in the presence of magnetic field. The magnetic field is $\hbar\omega_c/\varepsilon_F = 2 \times 10^{-4}$ (solid line), 10×10^{-4} (broken line), and 30×10^{-4} (dotted line). The other parameters are the same as in Fig. 10.

conductance increases, becomes maximal, and decreases, in accordance with the analytical result in Sec. III B.

V. CONCLUSIONS AND DISCUSSION

We have studied the mechanism of SHE at a QD with discrete energy levels in multiterminal geometries. We have considered a QD with SO interaction connected to N external leads via tunnel barriers. When an unpolarized current is injected to the QD from a lead, a polarized current is ejected to others. $N \geqslant 3$ ($N \geqslant 2$) is required in the absence (presence) of magnetic field for the generation of spin-polarized current.

First, we have obtained the analytical expressions for the spin-dependent conductance using a minimal model of two-level QD. The SHE is markedly enhanced by the resonant tunneling when the level spacing in the QD is smaller than the level broadening due to the tunnel coupling to the leads. In the absence of magnetic field, the spin polarization can be tuned by changing the tunnel coupling to the lead other than source and drain leads in a three-terminal geometry. A weak magnetic field can tune the spin polarization in a two-terminal geometry. Second, we have performed numerical studies on the tight-binding model representing a QD with tunnel barriers to N leads. We have observed a large spin-polarized conductance at some current peaks when a few energy levels in the QD are close to each other around ε_F. The numerical results are in accordance with our analysis of the minimal model of two-level QD.

In our calculation, we have neglected the electron-electron interaction. Therefore, our theory is applicable only around the current peaks of the Coulomb oscillation, where the interaction is not qualitatively important. We have also neglected the Zeeman effect. In spite of a large g factor in InAs ($|g| \sim 10$),[20–23,26,27] the Zeeman effect is smaller than the orbital magnetization by one order of magnitude for $B \sim 40$ mT, as estimated in Appendix A. In the absence of SO interaction, the Zeeman effect would split a spin-degenerate level in the QD, which could result in the spin-polarized current by the resonant tunneling through one of the spin-split levels. In our situation, however, the spin splitting is much smaller than the level broadening, and hence the spin polarization by the Zeeman effect is negligibly small.

We discuss a possible observation of the SHE at a QD. Since the measurement of a spin-polarized current is usually difficult, an alternative method is desirable. Hamaya *et al.* fabricated InAs QDs connected to ferromagnets.[53] If a ferromagnet is used only for lead S and a normal metal or semiconductor is used for the other leads, an "inverse SHE" takes place. The electric current to lead D1 is proportional to $(1 + p\cos\theta)G_{1,+} + (1 - p\cos\theta)G_{1,-}$, where p is the polarization in the ferromagnet and θ is the angle between the magnetization and $\boldsymbol{h}_{SO}$. Thus, $G_{1,+}$ and $G_{1,-}$ can be evaluated by measuring the electric current with rotating the magnetization of the ferromagnet. The QDs are highly tunable systems. We believe that the detailed study of the generation of spin-polarized current at the QDs would contribute to the deeper understanding of the SHE.

ACKNOWLEDGMENTS

This work was partly supported by a Grant-in-Aid for Scientific Research from the Japan Society for the Promotion of Science, and by the Global COE Program "High-Level Global Cooperation for Leading-Edge Platform on Access Space (C12)." T.Y. is a Research Fellow of the Japan Society for the Promotion of Science.

APPENDIX A: APPROXIMATION IN WEAK MAGNETIC FIELD

In the presence of magnetic field and SO interaction, the Hamiltonian in Eq. (4) is approximated to that in Eq. (5) for the following reasons. We consider the situation in which the average of level spacing in the QD is $\delta \sim \hbar^2/(m^* d^2) \simeq 1$ meV, the strength of SO interaction is $\Delta_{SO} \simeq 0.2$ meV, and magnetic field of $\hbar\omega_c \sim \Delta_{SO}$ or smaller. Here, d is the one-dimensional size of the QD, effective mass $m^*/m_0 \simeq 0.024$ in InAs, and $\omega_c = |e|B/m^*$ is the cyclotron frequency.

We choose the gauge of $\boldsymbol{A} = (\boldsymbol{B} \times \boldsymbol{r})/2$ in the model of two-level QD. The first order in $\boldsymbol{A}$ in Hamiltonian (4) gives rise to the matrix element in Eq. (7). $|b| \sim \hbar\omega_c$, as denoted in Sec. II. The second order in $\boldsymbol{A}$ yields $e^2/(8m^*)\langle i|(\boldsymbol{B} \times \boldsymbol{r})^2|j\rangle \sim (eBd)^2/m^* = (\hbar\omega_c)^2/\delta$, which is smaller than the first-order term by $\hbar\omega_c/\delta \ll 1$. We also neglect the Zeeman effect $H_Z = g\mu_B \boldsymbol{B} \cdot \boldsymbol{\sigma}/2$, where $\mu_B = |e|\hbar/(2m_0)$ is the Bohr magneton. We estimate the effect to be $|g|\mu_B B/2 = (|g|/4)(m^*/m_0)\hbar\omega_c$. Since $|g| \sim 10$ in InAs,[20–23,26,27] the Zeeman term is smaller than the orbital magnetization $|b|$ by one order of magnitude.

In the presence of magnetic field, $\boldsymbol{p}$ in H_{SO} is replaced by $(\boldsymbol{p} - e\boldsymbol{A})$. In the case of Rashba interaction,

$$H_{RSO}(\boldsymbol{B}) = \frac{\lambda}{\hbar}[(\boldsymbol{p} - e\boldsymbol{A}) \times \nabla U] = \frac{\lambda}{\hbar}(\boldsymbol{p} \times \nabla U) - \frac{e\lambda}{2\hbar}[(\boldsymbol{B} \times \boldsymbol{r}) \times \nabla U]. \quad \text{(A1)}$$

The matrix element of the first term in Eq. (A1) is estimated to be $(\lambda/\hbar)|\langle 2|\boldsymbol{p} \times \nabla U|1\rangle| \sim (\lambda/d^2)\delta$, whereas that of the second term is to be $|e|\lambda/(2\hbar)|\langle i|(\boldsymbol{B} \times \boldsymbol{r}) \times \nabla U|j\rangle| \sim (|e|\lambda B/\hbar)\delta$. The latter is smaller than the former by a factor of $\hbar\omega_c/\delta \ll 1$, and thus it is safely disregarded. In the case of

Dresselhaus interaction,

$$H_{\mathrm{DSO}}(\boldsymbol{B}) = \frac{\lambda'}{\hbar}[(\pi_y\pi_x\pi_y - \pi_z\pi_x\pi_z)\sigma_x + (\pi_z\pi_y\pi_z - \pi_x\pi_y\pi_x)\sigma_y + (\pi_x\pi_z\pi_x - \pi_y\pi_z\pi_y)\sigma_z], \quad \text{(A2)}$$

where $\boldsymbol{\pi} = \boldsymbol{p} - e\boldsymbol{A}$. The matrix element of the terms without $\boldsymbol{A}$ [Eq. (2)] is estimated to be $(\lambda'\hbar^2/d^3)$ and that of the first order in $\boldsymbol{A}$ is to be $(\lambda'\hbar/d)|e|B$. Again, the latter is smaller than the former by a factor of $\hbar\omega_c/\delta \ll 1$.

APPENDIX B: NUMERICAL CALCULATION OF TIGHT-BINDING MODEL

In the model of Figs. 1(b) and 1(c), we discretize the xy plane with QPC potentials and obtain the two-dimensional tight-binding model of square lattice.[54] The lattice constant is denoted by a. For the region surrounded by the dotted line, the Hamiltonian is given by

$$H = t\sum_{j,l,\sigma}(4 + \tilde{U}_{j,l})c^\dagger_{j,l;\sigma}c_{j,l;\sigma} - t\sum_{j,l,\sigma}(T_{j,l;j+1,l;\sigma}c^\dagger_{j,l;\sigma}c_{j+1,l;\sigma} + T_{j,l;j,l+1;\sigma}c^\dagger_{j,l;\sigma}c_{j,l+1;\sigma} + \mathrm{H.\,c.}), \quad \text{(B1)}$$

where $c^\dagger_{j,l;\sigma}$ and $c_{j,l;\sigma}$ are creation and annihilation operators of an electron at site (j,l) with z component of spin $\sigma = \pm 1$, respectively. The transfer integral is $t = \hbar^2/(2m^*a^2)$. $\tilde{U}_{j,l}$ represents the QPC potential and electrostatic potential in the QD, at site (j,l) in units of t. The transfer term in the x direction is given by

$$T_{j,l;j+1,l;\pm} = \{1 \pm \mathrm{i}\tilde{\lambda}(\tilde{U}_{j+1/2,l+1/2} - \tilde{U}_{j+1/2,l-1/2})\}e^{\mathrm{i}2\pi\tilde{B}l}, \quad \text{(B2)}$$

where $\tilde{\lambda} = \lambda/(2a^2)$ is a dimensionless strength of SO interaction and $\tilde{U}_{j+1/2,l+1/2}$ is the potential at the middle point between the sites (j,l) and $(j+1,l+1)$. The magnetic field in the QD is taken into account by the Peierls phase factor $e^{\mathrm{i}2\pi\tilde{B}l}$ with $\tilde{B} = |e|Ba^2/h$. $\tilde{B}$ is related to the cyclotron frequency by $\tilde{B} = \hbar\omega_c/(4\pi t)$. The transfer term in the y direction is given by

$$T_{j,l;j,l+1;\pm} = 1 \mp \mathrm{i}\tilde{\lambda}(\tilde{U}_{j+1/2,l+1/2} - \tilde{U}_{j-1/2,l+1/2}). \quad \text{(B3)}$$

To randomize the discrete energy levels in the QD, we introduce a uniformly distributed onsite energy $w_{i,j}$ in the range of $-W_{\mathrm{ran}}/2 \leqslant w_{i,j} \leqslant W_{\mathrm{ran}}/2$. We choose $W_{\mathrm{ran}} = 0.2\varepsilon_F$. We disregard the SO interaction induced by the random potential.

The spin-dependent conductance is numerically evaluated in the following way. First, we define the channels in the leads outside of the dotted line, which are represented by the quantum wires of width $W = (M+1)a$. Consider a quantum wire in the x direction. There are M channels, M_{cond} of which are conduction modes and $(M - M_{\mathrm{cond}})$ are evanescent modes. The wave function of conduction mode μ ($\mu = 1,2,\ldots,M_{\mathrm{cond}}$) is written as

$$\psi_\mu(j,l) = \exp(\mathrm{i}k_\mu aj)u_\mu(l), \quad \text{(B4)}$$

$$u_\mu(l) = \sqrt{\frac{2}{M+1}}\sin\left(\frac{\pi\mu l}{M+1}\right), \quad \text{(B5)}$$

with $l = 0,1,2,\ldots,M$. The wave number k_μ satisfies $\varepsilon_\mu(k_\mu) = \varepsilon_F$, where the dispersion relation is given by

$$\varepsilon_\mu(k) = 4t - 2t\cos\left(\frac{\pi\mu}{M+1}\right) - 2t\cos(ka). \quad \text{(B6)}$$

The band edge $\varepsilon_\mu(k=0)$ is located below ε_F for the conduction modes. The wave function of evanescent mode μ ($\mu = M_{\mathrm{cond}}+1,\ldots,M$) is written as

$$\psi_\mu(j,l) = \exp(-\kappa_\mu aj)u_\mu(l), \quad \text{(B7)}$$

where aj is the distance from the end of lead. The band edge is located above ε_F and κ_μ is determined from $\varepsilon_\mu(\mathrm{i}\kappa_\mu) = \varepsilon_F$.

Next, we introduce the retarded Green's function $\hat{G}_\sigma(\varepsilon)$ for the inside region of the dotted line in Figs. 1(b) and 1(c). Here, $\sigma = \pm 1$ represents the z component of spin, which is a good quantum number in Hamiltonian (B1). It is defined by

$$\hat{G}_\sigma(\varepsilon) = \left[\varepsilon I - \mathcal{H}_\sigma - \sum_{\alpha=\mathrm{S,D}n}\Sigma_\alpha\right]^{-1}, \quad \text{(B8)}$$

where $\mathcal{H}_\sigma$ is the matrix of Hamiltonian with spin $\sigma = \pm$. Σ_α is the self-energy due to the tunnel coupling to lead $\alpha(=\mathrm{S,D}n)$ and given by

$$\Sigma_\alpha = -t\,\tau_\alpha^\dagger U\Lambda U^{-1}\tau_\alpha. \quad \text{(B9)}$$

$U = (\boldsymbol{u}_1,\boldsymbol{u}_2,\ldots,\boldsymbol{u}_M)$ is a unitary matrix, with $\boldsymbol{u}_\mu = [u_\mu(1),u_\mu(2),\ldots,u_\mu(M)]^{\mathrm{T}}$ in Eq. (B5). $\Lambda = \mathrm{diag}(\lambda_1,\lambda_2,\ldots,\lambda_M)$, where $\lambda_\mu = \exp(\mathrm{i}k_\mu a)$ for conduction modes and $\lambda_\mu = \exp(-\kappa_\mu a)$ for evanescent modes. τ_α is a coupling matrix to lead α; $\tau_\alpha(l,\alpha_l) = 1$ if site α_l is connected to the site l $(= 1,2,\ldots,M)$ at the end of the lead $\tau_\alpha(l,\alpha_l) = 0$ otherwise.[54] The conductance from lead S to D1 can be evaluated separately for $\sigma = \pm 1$ of the z component of spin. The spin-dependent conductance is calculated using the formula

$$G_{1,\pm} = \frac{4e^2}{h}\mathrm{Tr}[\Gamma_{\mathrm{D}1}\hat{G}_\pm(\varepsilon_F)\Gamma_{\mathrm{S}}\hat{G}^\dagger_\pm(\varepsilon_F)] \quad \text{(B10)}$$

at $T = 0$, where $\Gamma_\alpha = \mathrm{i}[\Sigma_\alpha - \Sigma^\dagger_\alpha]/2$.[54]

*tyokoyam@rk.phys.keio.ac.jp

[1] I. Žutić, J. Fabian, and S. Das Sarma, Rev. Mod. Phys. **76**, 323 (2004).

[2] E. I. Rashba, Fiz. Tverd. Tela (Leningrad) **2**, 1224 (1960) [Sov. Phys. Solid State **2**, 1109 (1960)].

[3] Yu. A. Bychkov and E. I. Rashba, J. Phys. C: Solid State Phys. **17**, 6039 (1984).

[4] When an electric field $\mathcal{E}$ is applied perpendicularly to two-dimensional systems in the xy plane ($V = e\mathcal{E}z$), Eq. (1) becomes a well-known form of $H_{\mathrm{RSO}} = (\alpha/\hbar)(p_y\sigma_x - p_x\sigma_y)$, where $\alpha = e\mathcal{E}\lambda$. In this paper, the term of Rashba interaction means a general form of Eq. (1).

[5] R. Winkler, *Spin-Orbit Coupling Effects in Two-Dimensional Electron and Hole Systems* (Springer, Berlin, 2003).

[6] J. Nitta, T. Akazaki, H. Takayanagi, and T. Enoki, Phys. Rev. Lett. **78**, 1335 (1997).
[7] G. Dresselhaus, Phys. Rev. **100**, 580 (1955).
[8] S. Murakami, N. Nagaosa, and S. C. Zhang, Science **301**, 1348 (2003).
[9] J. Wunderlich, B. Kaestner, J. Sinova, and T. Jungwirth, Phys. Rev. Lett. **94**, 047204 (2005).
[10] J. Sinova, D. Culcer, Q. Niu, N. A. Sinitsyn, T. Jungwirth, and A. H. MacDonald, Phys. Rev. Lett. **92**, 126603 (2004).
[11] M. I. Dyakonov and V. I. Perel, Phys. Lett. A **35**, 459 (1971).
[12] Y. K. Kato, R. C. Myers, A. C. Gossard, and D. D. Awschalom, Science **306**, 1910 (2004).
[13] H. A. Engel, B. I. Halperin, and E. I. Rashba, Phys. Rev. Lett. **95**, 166605 (2005).
[14] M. Eto and T. Yokoyama, J. Phys. Soc. Jpn. **78**, 073710 (2009).
[15] T. Yokoyama and M. Eto, Phys. Rev. B **80**, 125311 (2009).
[16] L. P. Kouwenhoven, C. M. Marcus, P. L. McEuen, S. Tarucha, R. M. Westervelt, and N. S. Wingreen, in *Mesoscopic Electron Transport*, NATO ASI Series E 345, edited by L. Y. Sohn, L. P. Kouwenhoven, and G. Schön (Kluwer, Dordrecht, 1997), p. 105.
[17] Y. Igarashi, M. Jung, M. Yamamoto, A. Oiwa, T. Machida, K. Hirakawa, and S. Tarucha, Phys. Rev. B **76**, 081303(R) (2007).
[18] C. Fasth, A. Fuhrer, L. Samuelson, V. N. Golovach, and D. Loss, Phys. Rev. Lett. **98**, 266801 (2007).
[19] A. Pfund, I. Shorubalko, K. Ensslin, and R. Leturcq, Phys. Rev. B **79**, 121306(R) (2009).
[20] S. Takahashi, R. S. Deacon, K. Yoshida, A. Oiwa, K. Shibata, K. Hirakawa, Y. Tokura, and S. Tarucha, Phys. Rev. Lett. **104**, 246801 (2010).
[21] Y. Kanai, R. S. Deacon, S. Takahashi, A. Oiwa, K. Yoshida, K. Shibata, K. Hirakawa, Y. Tokura, and S. Tarucha, Nat. Nanotechnol. **6**, 511 (2011).
[22] R. S. Deacon, Y. Kanai, S. Takahashi, A. Oiwa, K. Yoshida, K. Shibata, K. Hirakawa, Y. Tokura, and S. Tarucha, Phys. Rev. B **84**, 041302(R) (2011).
[23] M. D. Schroer, K. D. Petersson, M. Jung, and J. R. Petta, Phys. Rev. Lett. **107**, 176811 (2011).
[24] V. N. Golovach, M. Borhani, and D. Loss, Phys. Rev. B **74**, 165319 (2006).
[25] K. C. Nowack, F. H. L. Koppens, Yu. V. Nazarov, and L. M. K. Vandersypen, Science **318**, 1430 (2007).
[26] S. Nadj-Perge, S. M. Frolov, J. W. W. van Tilburg, J. Danon, Yu. V. Nazarov, R. Algra, E. P. A. M. Bakkers, and L. P. Kouwenhoven, Phys. Rev. B **81**, 201305(R) (2010).
[27] S. Nadj-Perge, S. M. Frolov, E. P. A. M. Bakkers, and L. P. Kouwenhoven, Nature (London) **468**, 1084 (2010).
[28] S. Nadj-Perge, V. S. Pribiag, J. W. G. van den Berg, K. Zuo, S. R. Plissard, E. P. A. M. Bakkers, S. M. Frolov, and L. P. Kouwenhoven, Phys. Rev. Lett. **108**, 166801 (2012).
[29] In two dimensions with an impurity potential, the SHE is weakened when the axial symmetry of the potential is broken; see T. Yokoyama and M. Eto, Physica E (Amsterdam) **42**, 956 (2010).
[30] M. Eto and T. Yokoyama, J. Phys. Soc. Jpn. **79**, 123711 (2010).
[31] A. A. Kiselev and K. W. Kim, Phys. Rev. B **71**, 153315 (2005).
[32] J. H. Bardarson, İ. Adagideli, and Ph. Jacquod, Phys. Rev. Lett. **98**, 196601 (2007).
[33] J. J. Krich and B. I. Halperin, Phys. Rev. B **78**, 035338 (2008).
[34] J. J. Krich, Phys. Rev. B **80**, 245313 (2009).
[35] E. N. Bulgakov, K. N. Pichugin, A. F. Sadreev, P. Středa, and P. Šeba, Phys. Rev. Lett. **83**, 376 (1999).
[36] A. A. Kiselev and K. W. Kim, Appl. Phys. Lett. **78**, 775 (2001).
[37] A. A. Kiselev and K. W. Kim, J. Appl. Phys. **94**, 4001 (2003).
[38] T. P. Pareek, Phys. Rev. Lett. **92**, 076601 (2004).
[39] M. Yamamoto and B. Kramer, J. Appl. Phys. **103**, 123703 (2008).
[40] B. K. Nikolić, L. P. Zârbo, and S. Souma, Phys. Rev. B **72**, 075361 (2005).
[41] T. Koga, J. Nitta, H. Takayanagi, and S. Datta, Phys. Rev. Lett. **88**, 126601 (2002).
[42] M. Eto, T. Hayashi, and Y. Kurotani, J. Phys. Soc. Jpn. **74**, 1934 (2005).
[43] P. G. Silvestrov and E. G. Mishchenko, Phys. Rev. B **74**, 165301 (2006).
[44] J. I. Ohe, M. Yamamoto, T. Ohtsuki, and J. Nitta, Phys. Rev. B **72**, 041308 (2005).
[45] A. Fert and O. Jaoul, Phys. Rev. Lett. **28**, 303 (1972).
[46] A. Fert, A. Friederich, and A. Hamzic, J. Magn. Magn. Mater. **24**, 231 (1981).
[47] G. Y. Guo, S. Maekawa, and N. Nagaosa, Phys. Rev. Lett. **102**, 036401 (2009).
[48] Y. Meir and N. S. Wingreen, Phys. Rev. Lett. **68**, 2512 (1992).
[49] In the presence of more than one conduction channel in the leads, a spin-polarized current can be generated in two-terminal systems without magnetic field, e.g., see Ref. 42.
[50] F. Zhai and H. Q. Xu, Phys. Rev. Lett. **94**, 246601 (2005).
[51] C. Karrasch, T. Hecht, A. Weichselbaum, Y. Oreg, J. von Delft, and V. Meden, Phys. Rev. Lett. **98**, 186802 (2007), and related references cited therein.
[52] T. Ando, Phys. Rev. B **44**, 8017 (1991).
[53] K. Hamaya, M. Kitabatake, K. Shibata, M. Jung, M. Kawamura, K. Hirakawa, T. Machida, T. Taniyama, S. Ishida, and Y. Arakawa, Appl. Phys. Lett. **91**, 022107 (2007).
[54] S. Datta, *Electronic Transport in Mesoscopic Systems* (Cambridge University Press, Cambridge, 1995).